scientific reports

Check for updates

OPEN

Inhibition of HIV-1 gene transcription by KAP1 in myeloid lineage

Amina Ait-Ammar[1,2,3], Maxime Bellefroid[3], Fadoua Daouad[1], Valérie Martinelli[4], Jeanne Van Assche[1], Clémentine Wallet[1], Anthony Rodari[3], Marco De Rovere[1], Birthe Fahrenkrog[4], Christian Schwartz[1], Carine Van Lint[3,5]✉, Virginie Gautier[2,5]✉ & Olivier Rohr[1,5]✉

HIV-1 latency generates reservoirs that prevent viral eradication by the current therapies. To find strategies toward an HIV cure, detailed understandings of the molecular mechanisms underlying establishment and persistence of the reservoirs are needed. The cellular transcription factor KAP1 is known as a potent repressor of gene transcription. Here we report that KAP1 represses HIV-1 gene expression in myeloid cells including microglial cells, the major reservoir of the central nervous system. Mechanistically, KAP1 interacts and colocalizes with the viral transactivator Tat to promote its degradation via the proteasome pathway and repress HIV-1 gene expression. In myeloid models of latent HIV-1 infection, the depletion of KAP1 increased viral gene elongation and reactivated HIV-1 expression. Bound to the latent HIV-1 promoter, KAP1 associates and cooperates with CTIP2, a key epigenetic silencer of HIV-1 expression in microglial cells. In addition, Tat and CTIP2 compete for KAP1 binding suggesting a dynamic modulation of the KAP1 cellular partners upon HIV-1 infection. Altogether, our results suggest that KAP1 contributes to the establishment and the persistence of HIV-1 latency in myeloid cells.

The pandemic of HIV-1 infections is a global health problem. Current cART (combination antiretroviral therapy) efficiently suppresses viral expression below clinical detection levels but fails to eradicate latently infected reservoirs, the main obstacles toward an HIV cure. Indeed, most efforts have focused on understanding latency molecular mechanisms in resting memory CD4+ T-cell reservoirs. However, they are not the only source of viral rebound. Myeloid cells such as monocytes, tissue-resident macrophages and follicular dendritic cells are part of the viral reservoir[1–3]. Protected by the blood brain barrier, the central nervous system is a major anatomic reservoir and a sanctuary for the virus[4]. Indeed, integrated SIV DNA have been reported in the CNS of infected macaques, with undetectable plasma viral load[5]. In the brain, microglial cells are the major reservoirs of latently integrated HIV-1[6]. The specific molecular mechanisms controlling HIV-1 gene silencing in these CNS resident macrophages should be taken into consideration to design strategies toward HIV cure.

We have previously reported the importance of the cellular co-factor CTIP2 (Coup-TF Interacting Protein 2) in the establishment of HIV-1 post-integration latency in microglial cells[7–9]. CTIP2 promotes and maintains HIV-1 gene silencing by recruiting chromatin modifying complexes including HDAC1/2 (Histone Deacetylase 1/2), SUV39h1 (Suppressor of Variegation 3–9 Homolog 1) and LSD1 (Lysine-Specific histone Demethylase 1A) to the viral promoter[9,10]. In addition, CTIP2 targets and represses HIV-1 Tat transactivation function by promoting its relocation to heterochromatin structure via the formation of a Tat-CTIP2-HP1α (Heterochromatin Protein 1α) complex[11] and by repressing the elongation factor P-TEFb[12]. P-TEFb is the key cofactor of Tat. CTIP2 associates with an inactive form of P-TEFb to repress the CDK9 (Cyclin Dependent Kinase 9) catalytic subunit and inhibit P-TEFb sensitive genes including HIV-1[12]. Finally, we reported that HMGA1 recruits this CTIP2-associated inactive P-TEFb complex to the viral promoter[13]. Importantly, Desplats et al., revealed that CTIP2

[1]Université de Strasbourg, UR 7292 DHPI, FMTS, IUT Louis Pasteur, 1 Allée d'Athènes, 67300 Schiltigheim, France. [2]Center for Research in Infectious Diseases (CRID), School of Medicine and Medical Science (SMMS), University College Dublin (UCD), Dublin, Ireland. [3]Service of Molecular Virology, Institute for Molecular Biology and Medicine (IBMM), Université Libre de Bruxelles (ULB), Gosselies, Belgium. [4]Laboratory Biology of the Nucleus, Institute for Molecular Biology and Medicine, Université Libre de Bruxelles, 6041 Charleroi, Belgium. [5]These authors jointly supervised this work: Carine Van Lint, Virginie Gautier and Olivier Rohr. ✉email: cvlint@ulb.ac.be; virginie.gautier@ucd.ie; olivier.rohr@unistra.fr

expression is increased in the CSF, astrocytes and microglial cells from PLWH (Patients Living With HIV) on suppressive cART[14]. Collectively, our results demonstrate the importance of CTIP2 and its partners in the regulation of HIV-1 gene silencing. The HIV-1 latency is a multifactorial phenomenon involving factors dedicated to epigenetic gene silencing. KAP1 (KRAB (Krugel-Associated Box) domain-Associated Protein 1), also known as TRIM28 (Tripartite Motif-containing Protein 28) or TIF1β (Transcriptional Intermediary Factor 1 beta) is one of them. It was identified in 1996 as an interaction partner of the KRAB-ZFPs (Krüppel-Associated Box Zinc Finger Proteins) transcription factors family members[15]. KAP1 is a protein with multiple functional domains that regulates the chromatin environment through interactions with different partners[16]. KAP1 is recruited to DNA loci via interactions of its RBCC (RING finger, 2 B-box zinc fingers, Coiled-Coil region) domain with KRAB proteins[17]. The RING domain of KAP1 has SUMO and Ubiquitin E3 ligase activities and induces heterochromatin structures[18–20], the PHD (Plant Homeo Domain) C-terminal domain has a SUMO E3 ligase activity needed to SUMOylate its own Bromo domain and the SUMOylated Bromo domain recruits the NURD and SETDB1 repressor complexes[21]. KAP1 is known to repress endogenous and latent retrovirus[22]. In HIV-1 infected cells, KAP1 associates with HDAC1 to deacetylate the integrase and inhibit proviral integration[23]. At the transcriptional level, KAP1 has been reported to contribute to ZBRK1 (Zinc finger and BRCA1 (Breast cancer type 1 susceptibility protein)-interacting protein with A KRAB domain 1) and ZNF10 (Zinc Finger Protein 10)-mediated HIV-1 LTR repression[24,25]. However, these studies have not yet shown the direct involvement of KAP1 and its mechanism of action. Moreover, KAP1-mediated recruitment of an inactive form of P-TEFb to most genes containing a paused RNA polymerase, including the HIV-1 LTR promoter to favor gene expression upon stimulation[26,27]. Despite these controversies, KAP1 is mainly shown as a viral gene repressor. KAP1 restricts the activation of MLV (Murine Leukemia Virus) and HTLV-1 (Human T-Lymphotropic Virus type 1) genes[28,29]. More recently, the restriction factor APOBEC3A (Apolipoprotein B mRNA-Editing enzyme Catalytic polypeptide-like 3G) has been described to recruit KAP1 to suppress HIV-1 transcription[30]. In addition, a recent study suggests that KAP1 represses HIV-1 gene expression by mediating CDK9 SUMOylation resulting in P-TEFb repression in T cells[31]. Surprisingly, since KAP1 functions have been extensively studied in T lineage, nothing has been done to define its role and its mechanism of action on HIV-1 infection in myeloid cells.

Here, we studied the influence of KAP1 on HIV-1 expression and its specific mechanism of action in monocytic and microglial cells, the resident macrophages and the main viral reservoirs in the brain. In microglial cells KAP1 repressed HIV-1 gene expression. While KAP1 was found associated with the silenced HIV-1 promoter in the CHME5-HIV microglial model of latency, stimulations released KAP1 from the provirus. RNA interference-mediated knockdown of KAP1 in monocytic cell line latently infected with HIV-1 showed an increase in viral reactivation and transcription. Mechanistically, KAP1 repressed the HIV-1 promoter activity in the absence and in the presence of the viral transactivator Tat. Moreover, KAP1 had a major repressive impact on Tat function. We report that KAP1 interacts physically and colocalizes with Tat in the nucleus of microglial cells to promote its degradation via the proteasome pathway. Finally, KAP1 was found associated with the repressor CTIP2. They both cooperated to repress Tat function. Altogether our results highlight the contribution and the specific mechanism of action of KAP1 in the establishment and the persistence of HIV-1 post-integration latency in cells from myeloid origin.

Results

KAP1 cooperates with CTIP2 to repress HIV-1 gene expression in microglial cells. The functional impact of KAP1 overexpression or depletion on HIV-1 gene expression was examined on microglial cells expressing the pNL4-3 Δ ENV Luc HIV molecular clone (Fig. 1A,B) or the episomal vector LTR-Luc (Fig. 1C,D). In both cases we observed that expression of increasing amounts of KAP1 inhibited the HIV-1 promoter activity in a dose-dependent manner, while KAP1 depletion stimulated its activity.

These results are consistent with a transcriptional control of the viral expression by KAP1 and support a repressive role of KAP1 on HIV-1 gene expression. Of note, KAP1 protein expression levels were assessed by Western blot and quantified (Figs. 1E,F). Given KAP1 capacity to silence HIV-1 gene expression, we next examined the presence of KAP1 at the silenced viral promoter in CHME5-HIV microglial model of HIV-1 latency[32]. Chromatin IP experiments using 5′LTR specific primers revealed the presence of KAP1 associated with the silent 5′LTR region of the provirus (Fig. 2A). However, treatments with TNFα and HMBA to induce viral reactivation significantly displaced KAP1 from the promoter (Fig. 2A). The activation of HIV-1 promoter was validated by increased binding of the RNA Pol II (Fig. 2A) and by quantification of the GFP positive cells (Fig. 2B). Our results suggest that KAP1 targets the latent viral promoter to promote HIV-1 post-integration latency in microglial cells. To confirm these results in other models of infected myeloid cells, we took advantage of THP89 cells latently infected with recombinant p89.6 HIV-1 reporter virus wherein the GFP gene is inserted in the viral genome[33]. We generated THP89 monocytic cell lines expressing nontarget (shNT) or KAP1 (shKAP1) small hairpin (sh) RNAs. The efficiency of KAP1 knockdown in the selected puromycin resistant cells was validated by Western blot (Fig. 3A). Using these cells, we assessed the role of KAP1 in viral latency and reactivation by monitoring GFP expression. Flow cytometry analysis and GFP transcripts quantifications revealed an increase of GFP positive cells upon KAP1 knockdown (Fig. 3A,B). Activation of HIV-1 gene transcription in THP89 cells following KAP1 depletion was further studied by quantifying initiated transcripts (TAR region), elongated transcripts (*gag* and *tat* regions), and the multiply spliced transcripts (Ms RNA) (Fig. 3C). Significant higher levels of elongated and multiply-spliced transcripts were observed in KAP1 knocked-down cells. Altogether, our results indicate that KAP1 depletion enables the release of HIV-1 transcriptional blocks underlying latency.

We have previously reported the importance of the cellular cofactor CTIP2 in the establishment and the persistence of HIV-1 latency[9,10,13]. Since KAP1 and CTIP2 have been both involved in the control of HIV-1 gene expression, we next investigated whether they interact functionally. We observed that overexpressing KAP1

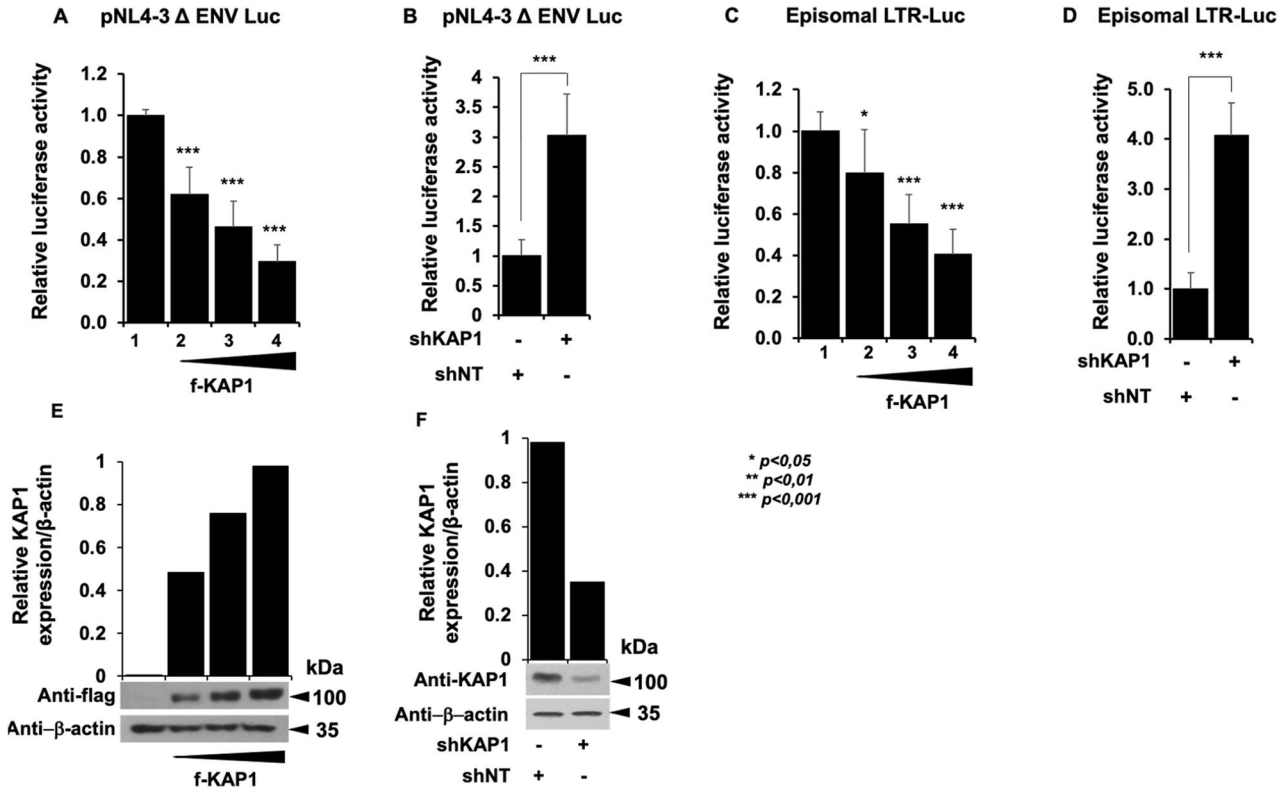

Figure 1. KAP1 suppresses HIV-1 expression (**A**–**D**) Microglial cells were transfected with the pNL4-3 Δ ENV Luc vectors (**A**,**B**) or with episomal vector LTR-Luc (**C**,**D**) in the presence of an increasing dose of KAP1 (**A**,**C**), or with a KAP1 knockdown (shKAP1) (**B**,**D**). Luciferase activity was measured 48 h post-transfection and after lysis of the cells. Luciferase values were normalized to those obtained with LTR-Luc or pNL4-3 Δ ENV Luc alone. A t-test was performed on 3 independent experiments *P* (**P* < 0.05, ***P* < 0.01, ****P* < 0.001). (**E**,F) Overexpressions of KAP1, as well as knockdown efficiencies, were validated by Western blotting. KAP1 expression levels were quantified and presented relatively to β-actin expression, using image J software. Full-length blots are presented in Supplementary Figure 1.

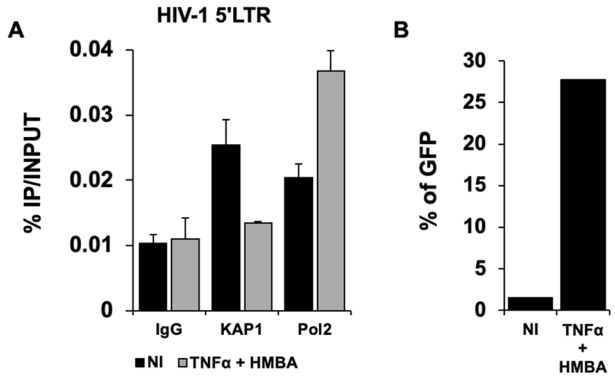

Figure 2. KAP1 binds to the latent HIV-1 promoter (**A**) Microglial cells latently infected with HIV-1 containing the GFP reporter gene were treated for 24 h with TNFα and HMBA. Cells were subjected to ChIP-qPCR experiments targeting the binding to the HIV-1 5′LTR promoter (**B**) The same microglial cells were also analyzed by flow cytometry. The results are presented as percentages of immunoprecipitated DNA compared to the input DNA (% IP/INPUT). This figure is representative of 3 independent experiments.

and CTIP2 had a stronger repressive activity on the HIV-1 provirus than overexpressions of each protein alone (Fig. 4A, column 4 versus 2 and 3). Similarly, we observed a modest but significant cooperation in the context of a simultaneous depletion of the two proteins (Fig. 4B, column 4 versus 2 and 3). As shown in Fig. 4C,D, similar results were obtained upon analysis of the activity of 5′LTR viral promoter. To ensure that the effects can be correlated to the expression levels of CTIP2 and KAP1, we performed Western blot analysis. The results demonstrated the efficiencies of the overexpression and the knockdown at the protein level (Figs. 4E,F). Since

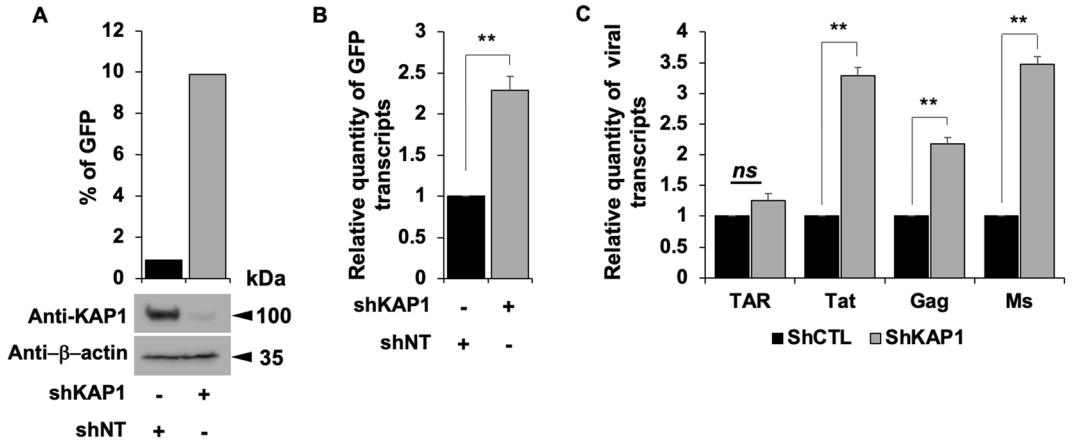

Figure 3. Reactivation of HIV-1 gene transcription in myeloid models of latency upon KAP1 depletion (**A**–**C**) The HIV-1 infected monocytic (THP89) cells containing a GFP reporter gene were transduced either with non-targeting shRNA (indicated as shNT) or shKAP1. (**A**) The GFP expression was examined by flow cytometry and the KAP1 protein expression level was assessed on total cellular extract by Western blot. (**B**,**C**) Total RNA products from shNT or shKAP1 THP89 transduced cells were retrotranscribed. GFP and HIV-1 gene transcripts as Initiated (TAR region), elongated (*gag*, *tat*), and multiple-spliced RNA (Ms RNA) were quantitated by real-time RT–PCR. The relative mRNA level was first normalized to GAPDH then to the shNT-transduced condition. Results are means from duplicate. Full-length blots are presented in Supplementary Figure 2.

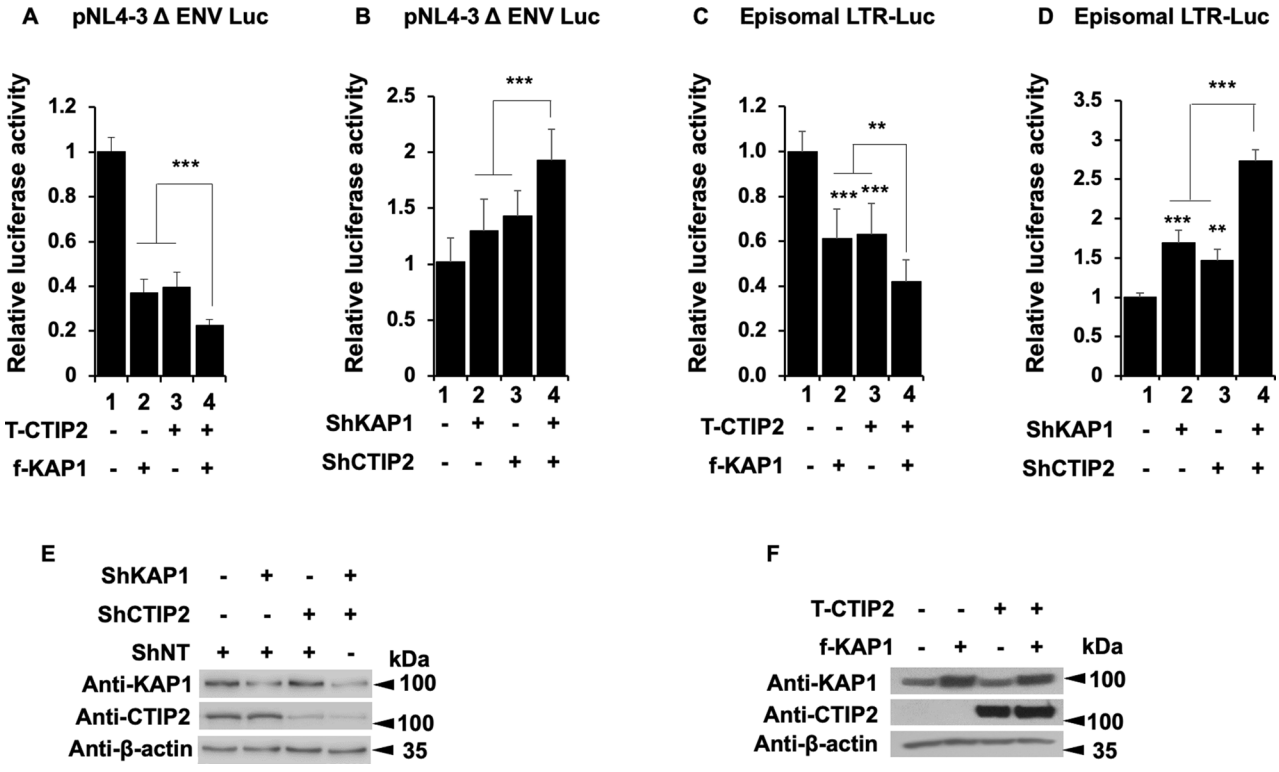

Figure 4. Kap1 and CTIP2 together contribute to the silencing of HIV-1 gene expression (**A**–**D**) Microglial cells were transfected with the pNL4-3 Δ ENV Luc vectors (**A**,**B**) or LTR-Luc (**C**,**D**) under the indicated conditions. The cells were lysed after 48 h of transfection. The luciferase activities were measured and normalized to the conditions where the pNL4-3 Δ ENV Luc and LTR-Luc vectors were transfected alone. A t-test was performed on 3 independent experiments *P* (**P* < 0.05, ***P* < 0.01, ****P* < 0.001). (**E**,**F**) Over-expression and knockdown of the indicated proteins were validated by Western blot. Full-length blots are presented in Supplementary Figure 3.

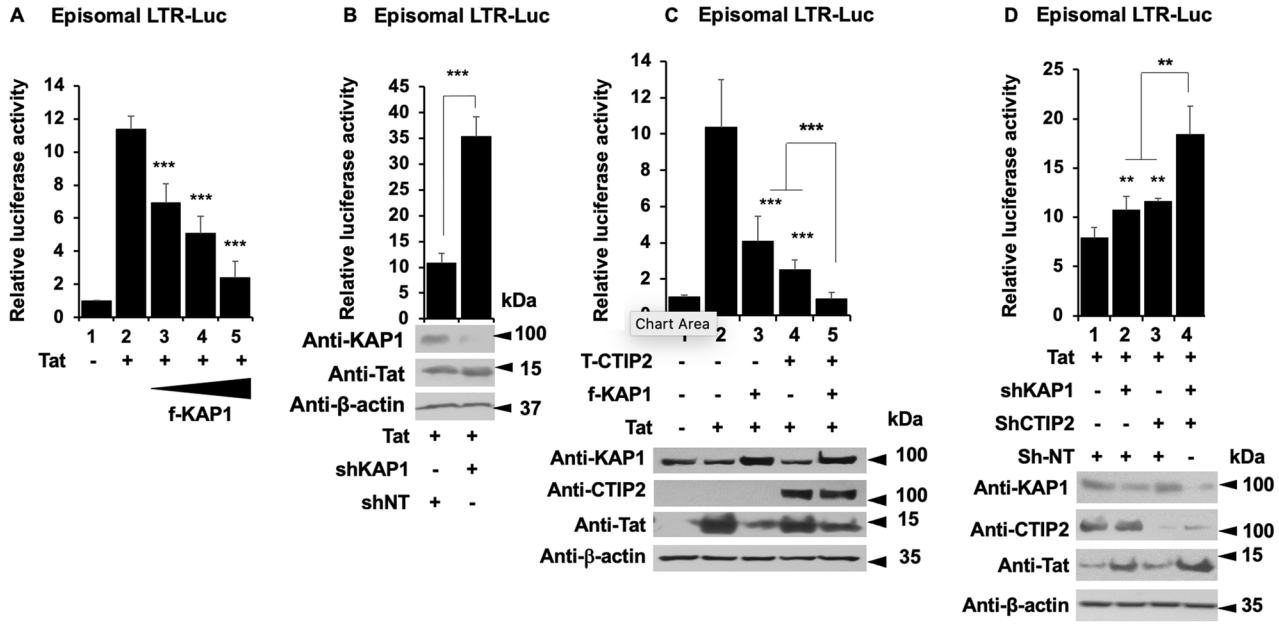

Figure 5. KAP1 inhibits Tat activity and cooperates with CTIP2 for this purpose (**A**–**D**) Microglial cells were transfected with LTR-Luc vector under the indicated conditions. After 48 h of transfection, the luciferase activities were measured after cell lysis and normalized under conditions where LTR-Luc vector were transfected alone. A t-test was performed on 3 independent experiments *P* (**P* < 0.05, ***P* < 0.01, ****P* < 0.001). (**C**,**D**) Over-expression and knockdown of the indicated proteins were validated by Western blot. Full-length blots are presented in Supplementary Figure 5.

KAP1 has been shown to promote the formation of heterochromatin environments[34], we investigated the role of KAP1 on H3K9me3 and HP1 recruitments at the HIV-1 promoter. As shown in supplementary figure 4, KAP1 depletion reduced H3K9me3 and HP1β but not HP1α bindings at the 5′LTR.

We have reported that CTIP2 represses Tat function by inducing its relocation in heterochromatin structures[11]. We therefore investigated the impact of KAP1 on Tat function. As expected, Tat expression stimulated the viral promoter activity (Fig. 5A, column 2). However, while the overexpression of KAP1 repressed this transactivation (Fig. 5A, columns 3 to 5 versus 2), the knockdown of KAP1 promoted Tat activity (Fig. 5B). These results confirmed that KAP1 regulates the initiation (−Tat) and the elongation (+Tat) steps of HIV-1 gene transcription. We next modulated the expression of KAP1 together with CTIP2. As expected, overexpression of KAP1 and CTIP2 alone inhibited Tat function (Fig. 5C, column 3 and 4). Moreover, their concomitant overexpression further repressed Tat-mediated activity (Fig. 5C, column 5). Logically, the concomitant depletion of KAP1 and CTIP2 favored Tat-mediated transactivation (Fig. 5D). As shown in Fig. 5C,D, the efficiencies of the overexpression and the depletions were controlled by Western blot. Taken together, our results demonstrate that KAP1 and CTIP2 cooperate functionally to repress HIV-1 gene expression in microglial cells.

KAP1 interacts and colocalizes with Tat. We have shown that KAP1 inhibits Tat function. In addition, we found that KAP1 cooperates with CTIP2 in Tat repression. These results prompted us to investigate a physical association of KAP1 with Tat. We performed co-immunoprecipitation targeting ectopically expressed KAP1 (Fig. 6A) and endogenously expressed KAP1 (Fig. 6B). As shown, Tat associates with KAP1 in both conditions. To next visualize the association of KAP1 and Tat in the nucleus, microglial cells expressing GFP-KAP1 and DsRed-Tat were analyzed by direct fluorescence microscopy. As previously described in the literature, KAP1 was found in the nucleoplasm and excluded from the nucleoli (Fig. 6C upper panel)[35]. In DsRed-Tat expressing cells, Tat is localized in both nucleoplasm and nucleoli (Fig. 6C, middle panel)[36,37]. In cells expressing GFP-Kap1 and DSRed-Tat, we observed that Tat colocalizes with KAP1 in the nucleoplasm but not in the nucleoli, (Fig. 6C, lower panel). GFP-KAP1 recruited Tat in KAP1-induced structures as shown by the yellow staining.

KAP1 promotes Tat degradation by the proteasome pathway. To further characterize mechanistically the repression of Tat by KAP1, we observed the pattern of Tat expression in the presence of increasing amount of KAP1 (Fig. 7A). We found that Tat expression was inversely correlated to the protein level of KAP1 upon KAP1 overexpression (Fig. 7A) and KAP1 depletion (Fig. 7B). To determine if these modulations of Tat protein expression are controlled post-transcriptionally, we quantified Tat mRNAs by RT-qPCR, in the presence or lack of KAP1 overexpression. Since the amount of Tat mRNA remained unaffected by KAP1 (Fig. 7C), we hypothesized that KAP1 overexpression leads to Tat depletion by regulating the stability of the protein. Among the mechanisms controlling protein half-life in eukaryotic cells, the degradation via the proteasome pathway has been long studied. Interestingly, Tat was previously described to be directed towards proteasome degradation[38–43]. To determine whether the reduced expression of Tat in the presence of KAP1 is related to pro-

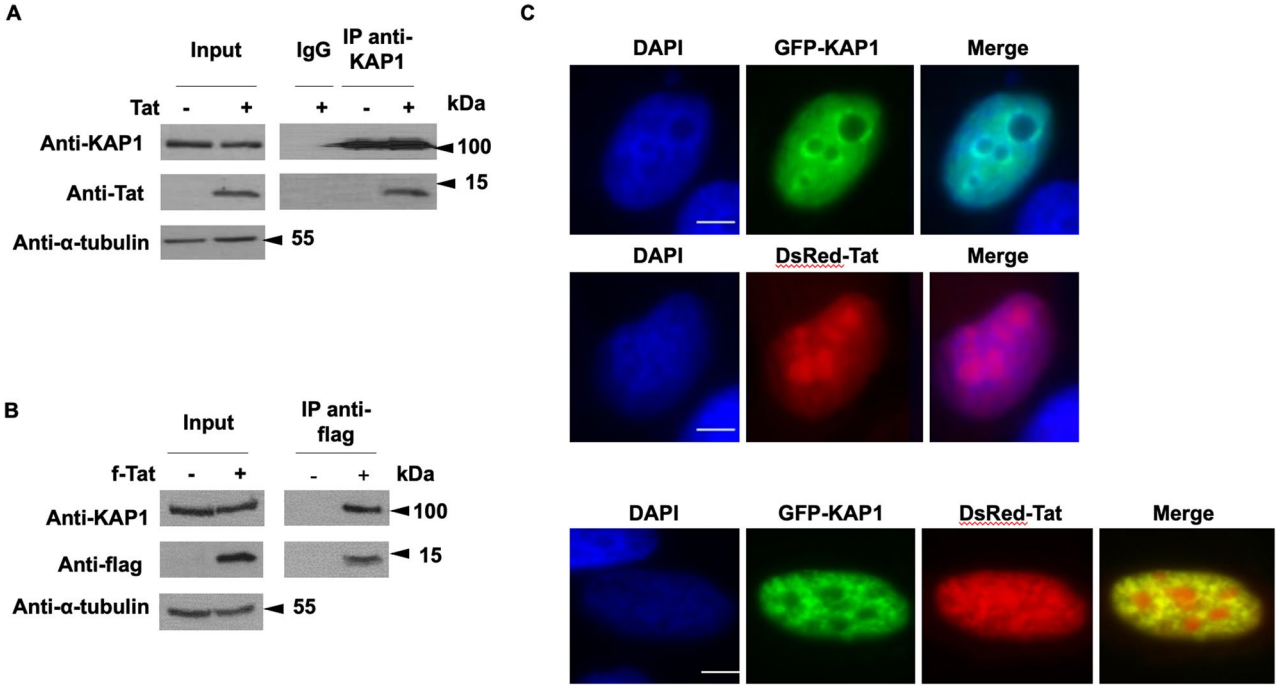

Figure 6. KAP1 interacts and colocalize with Tat (**A**,**B**) HEK cells were transfected with the indicated vectors. After 48 h of transfection, the nuclear protein extracts were immunoprecipitated with KAP1 (**A**) and flag (**B**) antibodies. The eluted protein complexes were analyzed by Western blotting for the presence of the indicated proteins. (**C**) Microglial cells were transfected for 48 h with the indicated vectors and subjected to observation under a fluorescence microscope. Scale bars are set to 5 µm. Full-length blots are presented in Supplementary Figure 6.

teasome degradation, we quantified Tat expression levels in the presence of KAP1 and the proteasome inhibitor MG132, (Fig. 7D). As expected, in the absence of MG132, KAP1 expression reduced significantly Tat expression (Fig. 7D, column 2 versus 1). However, MG132 treatment increased Tat protein levels by about 30% (Fig. 7D column 3 versus 1) and counteracted KAP1-mediated degradation of Tat (Fig. 7D, column 4 versus 2). Thus, our results suggest that KAP1 targets Tat to degradation via the proteasome pathway. Additional experiments performed with the inhibitor of translation Cycloheximide and the proteasome inhibitor Carfilzomib[44] further confirmed that KAP1-mediated depletion of Tat does not occur at the translation step but needs an active proteasome pathway (supplementary figure 8).

Tat degradation is mediated by the Bromo domains of KAP1. Using different KAP1 deletion mutants, we next identified the KAP1 domain required for Tat degradation (Fig. 7E). While deletion of the RBCC domain (ΔRBCC) did not affect KAP1-mediated degradation of Tat (Fig. 7E, column 3), deletions of the Bromo domain (Δ Bromo) and, at a lesser extent, of the PHD domain (ΔPHD) impaired Tat degradation (Fig. 7E, columns 4, 5 and 6 versus 2). We next used two mutants of KAP1, one mimicking a constitutive phosphorylation of Serine 824 (S824D) and the second which results in a non-phosphorylated form of KAP1 (S824A) (Fig. 7F). Of note, the phosphorylated status of the Serine 824 (located in the Bromo domain) determines the repressive activity of KAP1 and its ability to interact with the NuRD and SETDB1 repressor complexes via the Bromo domain[45]. While expression of KAP1 S824A promoted the degradation of Tat (Fig. 7F, column 5 versus 2), the S824D mutant did not (Fig. 7F, column 4). Overall, these results suggest that KAP1-mediated degradation of Tat may be regulated by phosphorylation of Serine 824 and thereby by the balance between the phosphorylated activating—and the dephosphorylated repressive forms of KAP1.

CTIP2 is interacting with KAP1 and competes with Tat for KAP1 binding. We demonstrated that KAP1 functionally cooperates with CTIP2 to inhibit HIV-1 gene expression. Since both CTIP2 and KAP1 have been reported to be associated with an inactive form of P-TEFb, we hypothesized that their functional interactions may result from physical association[12,26]. Immunoprecipitations targeting CTIP2 demonstrate that KAP1 associates with CTIP2 in RNA independent manner (Fig. 8A, column 4 and 6). Similar results were obtained after KAP1 immunoprecipitation (Fig. 8B, column 8 and 10) in the context of ectopic protein expression. We next confirmed these observations by immunoprecipitations targeting the endogenous proteins (Fig. 8C). To delineate the interface between KAP1 and CTIP2, we used different truncations of KAP1 and CTIP2 (Fig. 8D,E). We found that CTIP2 interacts with ΔPHD, ΔBromo, ΔPHD/ΔBromo deleted KAP1 (Fig. 8D, columns 10, 11, 12), but not with the ΔRBCC KAP1, (Fig. 8D, column 9). On the other hand, KAP1 binds only the 1-354 and 145-434 truncated forms of CTIP2 (Fig. 8E, column 11 and 12). Altogether, we found that the RBCC domain

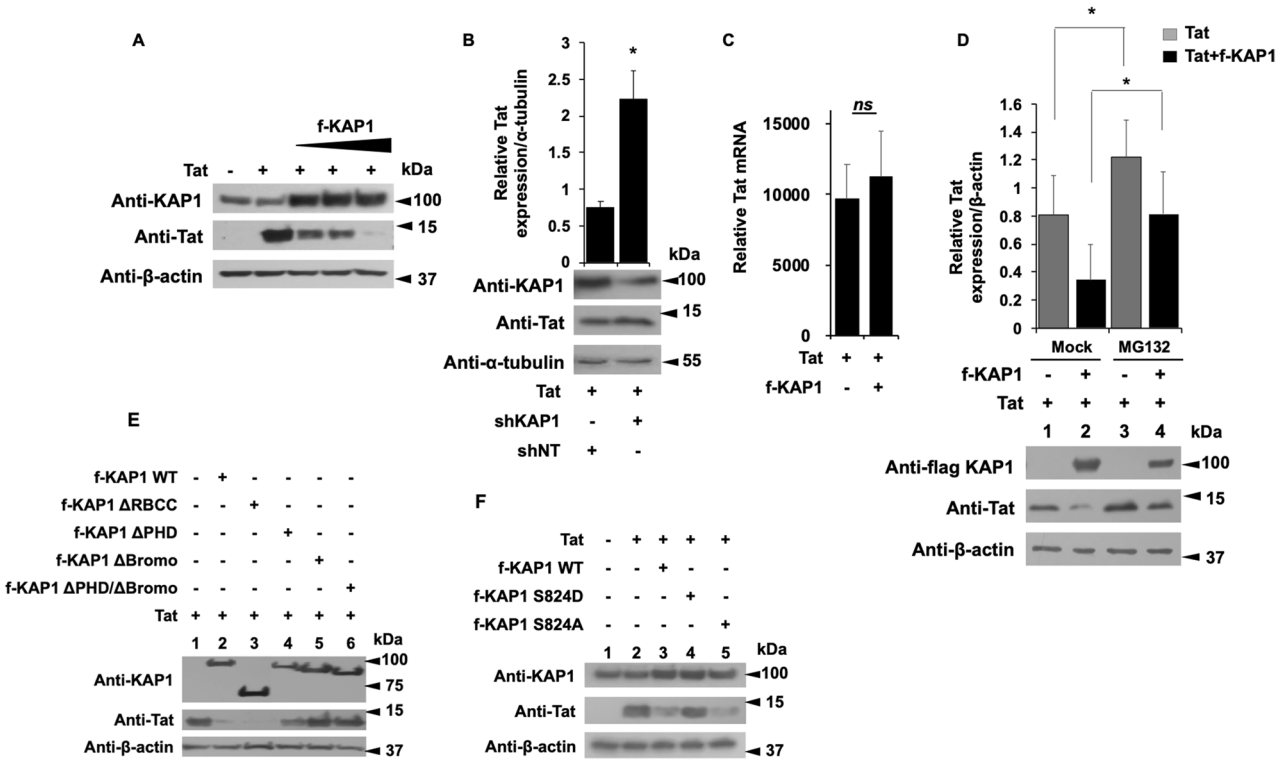

Figure 7. The Bromo domain of KAP1 promotes Tat degradation via the proteasome pathway (**A**,**B**,**E**,**F**) HEK cells were transfected with the indicated vectors. 48 h later, the nuclear proteins were analyzed by Western blot for the presence of the indicated proteins. (**B**) Tat expression level whose relative quantification to the α-tubulin was carried out using the image J software. (**C**) The RNA extracts from HEK cells transfected with the indicated plasmids were submitted to RT-qPCR experiments against Tat. The relative mRNA level of Tat was normalized to the GAPDH gene. (**D**) HEK cells were transfected with the indicated vectors. After 18 h of transfection, the cells were treated or not with 50 μM of MG132 for 6 h. 24 h post-transfection, the total protein extracts were analyzed by Western blot for the presence of KAP1 and Tat. Tat expression level was quantified relatively to β-actin expression, using image J software. A t-test was performed on 3 (**B**,**C**) and 5 (**D**) independent experiments *P* (**P* < 0.05, ***P* < 0.01, ****P* < 0.001). Full-length blots are presented in Supplementary Figure 7.

of KAP1 associated with the central region of CTIP2 previously shown to mediate Tat binding[11]. The interface between the central region of CTIP2 (amino acid residue144-354) and the RBCC domain of KAP1 (amino acid residue 65-376) is indicated by red lines in Fig. 8F. It should be noted that Tat has an additional CTIP2 binding site located at its C-terminal domain, between residues 717 and 813[11]. Co-immunoprecipitation experiments carried out with nuclear extracts expressing CTIP2, KAP1 and increasing amount of Tat, showed that Tat expression displaced CTIP2 from KAP1 suggesting that Tat may have a better affinity for KAP1 than CTIP2, (Fig. 8F, column 9 and 10).

Discussion

Antiretroviral therapy has significantly improved the management of HIV-1 infection. However, despite ART efficiency, it is still impossible to cure HIV-1 infected patients. Latently infected reservoirs are the major hurdles toward an HIV cure. Among the major reservoirs are the resting CD4+ T cells and monocyte-macrophage lineage, including microglial cells. These reservoirs escape immune surveillance and cannot be targeted by current therapies. HIV-1 gene transcription is silenced by epigenetic modifications. These epigenetic changes remain a major obstacle to virus eradication and patients cure. We have previously shown that CTIP2 is a major player in the establishment and persistence of HIV-1 latency in microglial cells[9,10,12]. In the present work we report the role and the mechanism of action of KAP1 as new partner of CTIP2 in the control of HIV-1 expression in myeloid cells. Functionally, KAP1 suppressed HIV-1 expression and contributed to viral latency in myeloid cells. In accordance, we found KAP1 associated with the latent HIV-1 promoter but not after reactivation. Interestingly, in CD4+ T cells, KAP1 binding to the HIV-1 promoter has been reported to be unsensitive to reactivations[31]. These controversies suggest that the mechanisms underlying KAP1 functions may be cell type specific. It is now well established that the repressive form of KAP1 is SUMOylated on its Bromo domain[46] and associates with the NuRD and SETDB1 repressor complexes (reviewed in[47]). The repressors CTIP2 and KAP1 have multiple similarities. They both interact with the NuRD complex[48,49], the DNA repair enzymes PARP1 and PRKDC[50,51] and a repressive form of P-TEFb complex including the 7SKsnRNP[26]. CTIP2 and KAP1 have also common target genes like p21[45,52]. Our results demonstrate a functional cooperation between the two repressors to repress HIV-1 gene transcription. KAP1 promotes a repressive chromatin environment at the viral promoter as previously

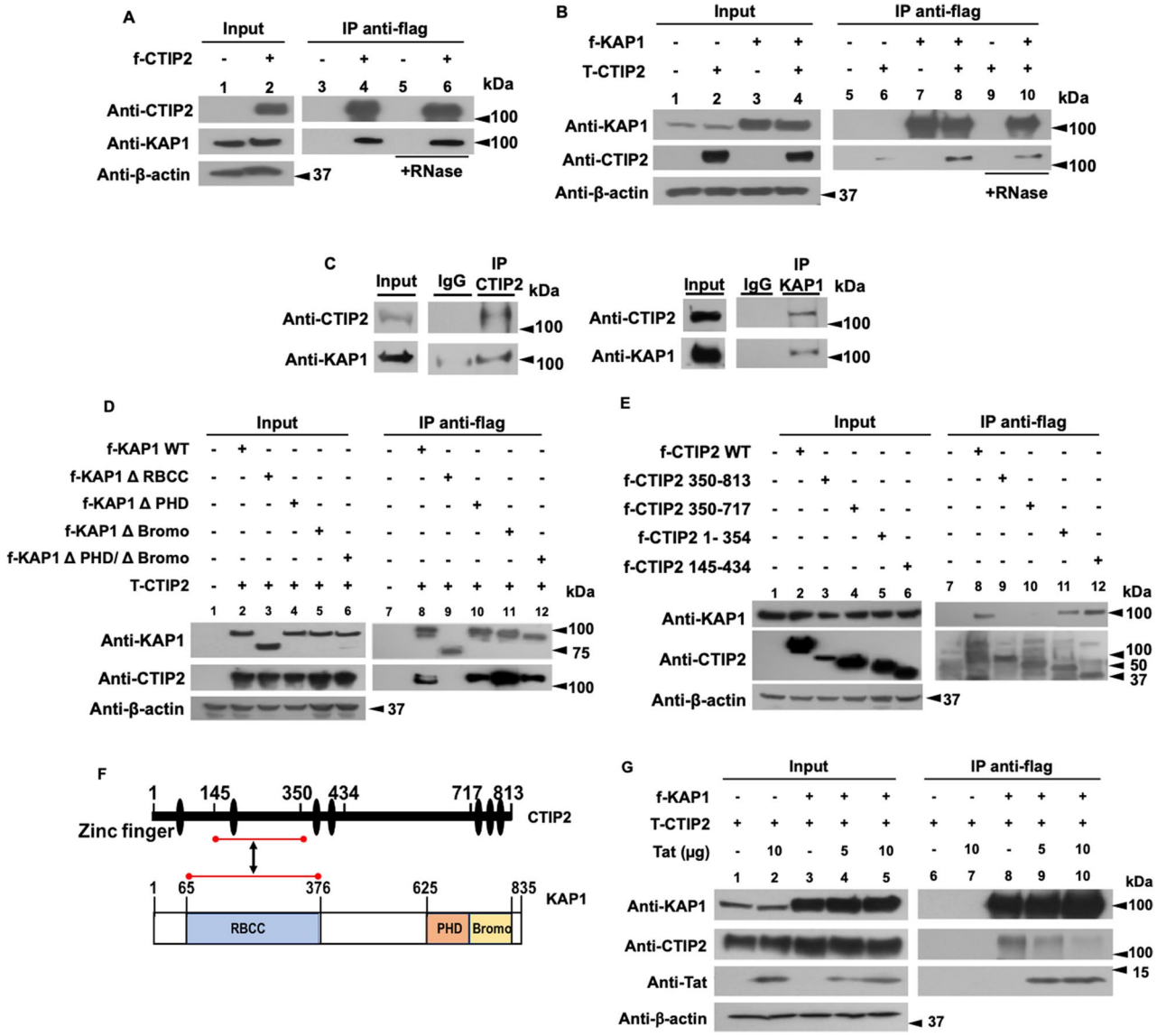

Figure 8. CTIP2 interacts with KAP1 in an RNA independent manner and competes with Tat for KAP1 binding (**A**,**B**) HEK cells were transfected with flag-CTIP2 (**A**) or flag-KAP1 and Tap-CTIP2 (**B**). 48 h post-transfection, the nuclear protein extracts, treated or not with RNase, were subjected to immunoprecipitation with the flag antibody. The immunoprecipitated complexes were tested by Western blot for the presence of KAP1 (**A**) and CTIP2 (**B**). (**C**) The nuclear protein extracts of microglial cells were analyzed by Western blot for the expression of CTIP2 and KAP1 and submitted to immunoprecipitation experiments with CTIP2 and KAP1 antibodies. (**D**) The HEK cells were transfected with Tap-CTIP2 and one of the vectors encoding f-KAP1 WT: wild type, or KAP1 deleted from the RBCC domain (ΔRBCC), or PHD (ΔPHD), or Bromo (ΔBromo) or both PHD and Bromo domains (ΔPHD/ΔBromo), or with f-CTIP2 deletion mutants, as indicated (**E**). After 48 h, the nuclear protein extracts were immunoprecipitated with flag antibody. The eluted protein complexes were analyzed by Western blot for the presence of CTIP2 and KAP1. (**F**) The interface between CTIP2 and KAP1 structural domains are presented. (**G**) HEK cells were transfected with the indicated vectors in the presence of an increasing dose of Tat. After 48 h, the nuclear protein extracts were treated as in (**D**). The results are representative of at least two independent experiments. Full-length blots are presented in Supplementary Figure 9.

shown for CTIP2[9]. Moreover, KAP1 and CTIP2 interact physically. We report that the RBCC domain of KAP1 associates with the central domain of CTIP2. CTIP2 association with LSD1 and HMGA1 has been described to inhibit Tat-dependent viral gene transcription and to promote its relocation in heterochromatin structures[10,11,13]. Our results show that KAP1 cooperates with CTIP2 to repress Tat function. In addition, we found that KAP1 interacts and colocalizes with Tat in the nucleoplasm of microglial cells. The HIV-1 Tat transactivator is essential to the elongation step of the viral gene mainly because of its ability to recruit P-TEFb at the HIV-1 initiated transcripts. Thereby, inhibiting Tat activity results in hindering the positive feedback loop required for efficient HIV-1

transcription. Interestingly, Tat has been shown to be sensitive to proteasome degradation[38–43,53]. We observed that Tat expression was inversely proportional to KAP1 expression level suggesting that KAP1-mediated repression of Tat function results from Tat degradation. KAP1 has been shown to promote proteasomal degradation of targets proteins by its RBCC domain[54–56]. Surprisingly, we observed that Tat degradation was not sensitive to RBCC depletion, weakly sensitive to PHD depletion, but mediated by the Bromo domain of KAP1. In line with these results, the point mutation of the KAP1 Serine 824 located in the Bromo domain abrogated Tat degradation. The Bromo domain is known to be modified by SUMOylation giving to KAP1 its repressive form. The phosphorylation of Serine 824 causes a loss of this SUMOylation state and a loss of KAP1 repressive activity[45]. Thus, our results suggest that Tat degradation is promoted by repressive SUMOylated forms of KAP1. Finally, we show that KAP1 interacts with Tat with higher affinity than with CTIP2. Indeed, upon increasing Tat expression, CTIP2 is displaced from KAP1 associated complex suggesting that the dynamic of KAP1 association with CTIP2 depends on the virological status of the cells. Altogether, our results suggest that KAP1 is a major player in the control of HIV-1 gene expression in microglial cells, the main HIV-1 reservoir in the brain. Moreover, they further highlight the cell type specific mechanism of action of the repressors involved in viral latency. CTIP2 and KAP1 are highly expressed in resting T cells and depleted upon activation[31,57]. In addition, increased levels of CTIP2 are associated with persistence of HIV-1 latency in the brain[14] and increased level of KAP1 in the peripheral blood of gastric cancer patients is a biomarker predicting cancer stage progression[58–61]. By transposition to what has been observed in oncology and virology, these repressors and their associated enzymatic activities may constitute good targets in therapies aiming at curing the HIV-1 infected patients.

Methods

Plasmids. The following plasmids: pcDNA3, flag CTIP2, flag-CTIP2 350-813, 350-717, 1-354 and 145-434, Tap-CTIP2, flag-Tat, DsRed-Tat, ShCTIP2, LTR-Luc, pNL4-3Δ Env Luc have been described previously[9,11,12]. The flag-KAP1 plasmids, flag-KAP1 S824A/D come from Dr. David K. Ann[45]. The vectors shKAP1 and shNT (non-target) were gift from Dr. Ivan D'orso[26]. The plasmids flag-KAP1WT, flag-KAP1 ΔRBCC, ΔPHD, ΔBromo, ΔPHD/ΔBromo were provided by Dr. Florence Cammas (IRCM Montpellier). GFP-KAP1 comes from Addgene (#65397).

Cell culture. The human microglial cell line (provided by Prof. M. Tardieu, Paris, France)[62], HEK293T cell lines and CHME5 cell lines latently infected with HIV-1[32] were maintained in Dulbecco's modifed Eagle medium (DMEM) containing 10% decomplemented fetal calf serum and 100 U/ml penicillin–streptomycin. When indicated, the cells were treated with 50 or 0.2 µM MG132 for 6 or 20 h respectively, with 50 µg/ml cycloheximide for 4 h and with 25 or 50 nM carfilzomib for 20 h. THP89 cell lines were grown in RPMI 1640 medium supplemented with 10% decomplemented fetal calf serum and 100 U/ml penicillin–streptomycin.

Antibodies and reagents. The list of antibodies and other chemical reagents used in this work are listed in Table 1.

Lentiviral production. HEK cells seeded at a density of 4×10^6 and grown in a 10 cm dish were transfected with the different shRNAs (shNT or shKAP1)-containing plasmids (9 µg), the pVSV-G (2.25 µg) and the psPAX2 (6.75 µg) packaging vectors by the calcium phosphate transfection method according to the manufacturer's protocol (TaKaRa; Calphos). 72 h post-transfection, the virus-containing supernatant (8 ml) was filtered (Steriflip; Merck) before being concentrated 20× (14,000 rpm, 1h30, 4°c) and stored at -80°c.

Generation of stable THP89 knock-down for KAP1. THP89 cells were transduced by spinoculation as previously described[26]. Briefly, 100 µl of 20× concentrated lentiviral stock was added to 10^6 cells previously washed and resuspended in 400 µl of complete growth medium containing polybrene (8 µg/ml). Cells were then centrifuged (3200 rpm 1 h, 32°c) before being incubated for 2 h at 37°c. After this incubation, cells were washed and transferred in 1 ml complete growth medium in a 12-well dish. 48 h post-infection, infected cells were selected by puromycin selection at a final concentration of 1 µg/ml for 2 weeks. GFP positive cells were measured by Flow Cytometry. Total proteins and RNAs were then extracted as described above for RT-qPCR and Western blotting.

Nuclear protein extract. Cells seeded at a density of 3×10^6 and grown in a 10 cm dish were transfected with the indicated vectors (30 µg) using the calcium phosphate coprecipitation method. 48 h post-transfection, cells were lysed for 10 min on ice in a buffer containing: 10 mM HEPES, 1.5 mM $MgCl_2$, 10 mM KCl and 0.5 mM DTT. After one minute of centrifugation at 13,000*g*, the nuclear pellet was lysed for 30 min on ice in another buffer containing: 20 mM HEPES, 25% glycerol, 1.5 mM $MgCl_2$, 420 mM NaCl, 0.2 mM EDTA, 0.5 mM DTT. After 2 min of centrifugation at 13,000*g*, the supernatant was analyzed by immunoprecipitation and Western blotting. Anti-proteases were systematically added to the lysis buffers.

Total protein extract. Cells seeded at a density of 0.5×10^6 cells per well and grown in a 6-well dish were transfected using the calcium phosphate coprecipitation method with the indicated vectors (12 µg). After 24 h, the cells were lysed on ice for 50 min using a buffer containing: 10 mM Tris HCl pH 7.5, 150 mM NaCl, 1 mM EDTA, 1% NP40, 0.5% Na deoxycholate, 0.1% SDS. After 10 min centrifugation at 13,000*g*, the supernatant was stored for Western blot analysis. Antiproteases were systematically added to the lysis buffers.

Reagent	Reference
Anti-CTIP2 antibody	A300-383A Bethyl
Anti-KAP1 antibody	Ab10483 Abcam
Anti-Tat antibody	ab43014 Abcam
Anti-β-actin antibody	A1978 Sigma-Aldrich
Anti-Flag antibody	F3165 Sigma-Aldrich
Anti-GFP antibody	632592 Clontech
Anti-α-tubulin antibody	Ab4074 Abcam
Anti-UBC9 antibody	610749 BD Biosciences
Anti-HA antibody	901 501 Biolegend
Anti-mouse IgG-HRP	Sc-358914 Santa Cruz
Anti-rabbit IgG-HRP	Sc-2004 Santa Cruz
Anti-KAP1 ChIP grade antibody	C15410236-100 Diagenode
Anti-RNA Pol II ChIP grade antibody	14958 Cell signaling
Anti-H3K9me3 ChIP grade antibody	1396 Cell signaling
Anti-HP1α ChIP grade antibody	2616 Cell signaling
Anti-HP1β ChIP grade antibody	8676 Cell signaling
anti-SP1 ChIP grade antibody	9389 Cell signaling
Rabbit IgG	C15410206 Diagenode
Mouse IgG	C15400001-15 Diagenode
Reverse PCR	1708890 Bio-Rad
Quantitative PCR	SsoAdvanced Universal SYBR Green Supermix – Bio-Rad
Anti-proteases	000000011873580001 Sigma-Aldrich
MG132	BML-PI102-0025 ENZO Life Sciences
Carfilzomib	AG-CR1-3669-M001 Bio-Connect
TNFα	300-01A PeproTech
HMBA	224235 Sigma-Aldrich
DMA	20660 Thermo Scientific
Anti-flag immunoprecipitation beads	A-2220 Sigma-Aldrich
Protein G magnetic beads	C03010021-220 Diagenode
Protein A magnetic beads	C03010020-220 Diagenode
Protein A Agarose/Salmon Sperm DNA	16-157 Sigma-Aldrich

Table 1. Antibodies and reagents.

Co-immunoprecipitation and Western blot analysis. Immunoprecipitations were performed on 500 µg of nuclear protein extracts using anti-flag M2 gel (Sigma-Aldrich) or by using Diagenode A/G protein-coupled magnetic beads to target endogenous proteins. Briefly, the nuclear protein extract was cleared for 1 h under rotation at 4 °C with the A/G protein-coupled magnetic beads. Meanwhile, the beads were coated under rotation with 1 µg of antibody for 30 min at room temperature. After the preclearing step, the beads were removed, replaced by the antibody coated beads and incubated overnight at 4 °C under rotation. The day after, the incubated beads were washed 2 times with a low salt buffer (50 mM TrisHCl pH 7.5, 120 mM NaCl, 0.5mMEDTA, 0.5% NP40, 10% glycerol), 2 times with a high salt buffer (50 mM TrisHCl pH 7.5, 0.5 M NaCl, 0.5 mM EDTA, 0.5% NP40, 10% glycerol) and one time with a low salt buffer. The immunoprecipitated proteins were eluted by heating at 100 °C during 15 min in 4 × Laemmli Sample Buffer (Bio-Rad). Immunoprecipitated protein complexes were subjected to Western blot analysis. The proteins were detected using the antibodies as indicated and visualized by a Thermo Scientific Chemiluminescence Detection System (Pierce-ECL Western Blotting Substrate 32106).

Fluorescence microscopy. The microglial cells were seeded at 0.8×10^6 and grown on coverslip in a 24-well plate. The cells were transfected after 24 h with the indicated vectors by the Jetprime (Polyplus transfection) method, according to the instructions of the supplier. After 48 h of transfection, the cells were fixed with PBS containing 2% formaldehyde for 15 min. The cells were then washed 3 times with PBS. The coverslip was mounted on a slide using the Mowiol 4-88 (Sigma-Aldrich) containing 1 µg/ml DAPI. Cells fluorescence was observed under a fluorescence microscope and imaged using a Zeiss Axio Observer inverted microscope (Zeiss, Oberkochen, Germany) with Zeiss Plan-Apochromat 100x/1.4 oil objective. Images were acquired using the microscope system software AxioVision V 4.8.2.0 and processed using Image J software.

Luciferase assay. Microglial cells, seeded at 0.4×10^6 in a 48-well dish, were transfected in triplicate by the calcium phosphate coprecipitation method with the indicated vectors. 48 h post-transfection, the cells were col-

Cellular model	Target	Forward primer	Reverse primer
HEK	*tat*	ACTCGACAGAGGAGAGCAAG	GAGATCTGACTGTTCTGATGA
	GAPDH	GGACCTGACCTGCCGTCTAGAA	GGGTGTCGCTGTTGAAGTCAGAG
THP89	TAR	GTTAGACCAGATCTGAGCCT	GTGGGTTCCCTAGTTAGCCA
	tat	TGTTGCTTTCATTGCCAAGCTTGTTT	GTCTTCGTCGCTGTCTCCGCT
	gag	AAAAGCATTGGGACCAGGAG	CTTGCTTTATGGCCGGGT
	Ms RNA	GGATCTGTCTCTGTCTCTCTCTCCACC	ACAGTCAGACTCATCAAGTTTCTCTATCAAAGCA
	GFP	GAGGGCGATGCCACCTAC	GGTGGTGCAGATGAACTTCAG

Table 2. PCR primers.

lected and the luciferase activity was measured using the Dual-Glo Luciferase Assay system (Promega Madisson, USA) and normalized to Renilla Luciferase activity.

Chromatin immunoprecipitation assay. Chromatin immunoprecipitation assay was performed following ChIP assay kit (EMD Millipore) protocol. Briefly, HIV-1 CHME5 cells were seeded at 3×10^6 in T175 Corning flask. 24 h later, the cells were mock treated or stimulated with 10 ng/ml of TNFα (Tumor Necrosis Factor α) and 5 mM of HMBA (Hexamethylene bisacetamide). After 24 h the cells were trypsinated, counted and then washed with PBS. THP89 transduced cells were seeded at 0.9×10^6 cell/ml. After 24 h the cells were, counted and then washed with PBS. In both conditions, the cells were resuspended at ratio of 4×10^6 cell/ml of PBS. The cells were cross-linked with a freshly made DMA (dimethyl adipimidate) at 5 mM for 25 min followed by a second 8 min cross-link with formaldehyde at 1%. The cross-linking reaction was stopped by 0.125 M of Tris–Glycine solution. Cells were washed twice with ice cold PBS then resuspended to a ratio of 10×10^6/300 µl of SDS Lysis buffer (Tris HCl 50 mM pH 8, EDTA 10 mM, 1% SDS) containing proteases inhibitors. The chromatin was sonicated (Bioruptor Plus, Diagenode) 40 min (30 s on, 30 s off) to obtain DNA fragments of 200–400 bp. Chromatin immunoprecipitations were performed with chromatin from 5×10^6 cells and 5 µg of antibodies. IgG was used as a control for immunoprecipitation. The DNA was purified using the High Pure PCR Product Purification Kit (11732676001 Sigma-Aldrich). Quantitative Real Time PCR reactions were performed with the TB Green Premix Ex Taq II (TAKARA) as recommended by the supplier. Relative quantification using standard curve method was performed for the primer pair, and 96-well plates (MU38900 Westburg) were read in a StepOnePlus PCR instrument (Applied Biosystems). The Results are presented as percentages of immunoprecipitated DNA compared to the input DNA (% IP/INPUT). The 5′LTR forward and reverse Primer sequences used are respectively: 5′-TGGAAAATCTCTAGCAGTGGC-3′, 5′-GAGTCCTGCGTCGAGAGATCT-3′ for CHME5 HIV-1 provirus and 5′-TCTCTAGCAGTGGCGCCCGA-3′, 5′-GCCCCTCGCCTCTTGCTGTG-3′ for THP89 HIV-1 provirus.

Flow cytometry. CHME5 HIV-1 cells mock treated or stimulated with 10 ng/ml of TNFα and 5 mM of HMBA for 24 h or either THP89 HIV-1 cells transduced with lentiviral particles were washed twice in PBS, resuspended in PBS containing 4% paraformaldehyde and fixed for 1 h at 4 °C in the dark. Cells were then washed twice in PBS and resuspended in FACS buffer (PBS, 0.1% BSA, 0.1% NaN_3). The percentage of GFP-positive cells was measured on a CXP cytometer (Cytomics FC 500, Beckman Coulter) using CXP Software version 1.0 according to the manufacturer's instructions.

mRNA quantification. Total RNA was extracted from cells expressing the indicated vectors according to the QIAGEN RNeasy Plus Kit protocol or with Tri-Reagent (TRC118, MRC) according to the manufacturer's instructions. Following DNAse treatment (AM1907, Invitrogen), the cDNAs were produced using Bio-Rad Reverse Transcription Kit (iScript Reverse Transcription Supermix) or the PrimeScript RT reagent kit (RR037A, TaKaRa). cDNAs from HEK and THP89 cells were quantified by quantitative PCR using Bio-Rad's SsoAdvanced Universal SYBR Green Supermix. Data were calculated using the $2^{-(\Delta\Delta CT)}$ method and normalized to the amount of GAPDH. The PCR primers used are presented in Table 2.

Statistical analysis. Data were analyzed by performing the student t-test using Microsoft Excel. Values of $p < 0.05$ (*), $p < 0.01$ (**) and $p < 0.001$ (***) were considered significant. The results were represented as mean and standard deviation of at least 3 independent experiments.

Received: 5 June 2020; Accepted: 13 January 2021
Published online: 29 January 2021

References

1. Kumar, A., Abbas, W. & Herbein, G. HIV-1 latency in monocytes/macrophages. *Viruses* **6**, 1837–1860 (2014).
2. Kandathil, A. J., Sugawara, S. & Balagopal, A. Are T cells the only HIV-1 reservoir?. *Retrovirology* **13**, 86 (2016).
3. Honeycutt, J. B. *et al.* HIV persistence in tissue macrophages of humanized myeloid-only mice during antiretroviral therapy. *Nat. Med.* **23**, 638–643 (2017).

4. Gelman, B. B. *et al.* Neurovirological correlation with HIV-associated neurocognitive disorders and encephalitis in a HAART-era cohort. *J. Acquir. Immune Defic. Syndr.* **62**, 487–495 (2013).
5. Clements, J. E., Gama, L., Graham, D. R., Mankowski, J. L. & Zink, M. C. A simian immunodeficiency virus macaque model of highly active antiretroviral treatment: Viral latency in the periphery and the central nervous system. *Curr. Opin. HIV AIDS* **6**, 37–42 (2011).
6. Llewellyn, G. N., Alvarez-Carbonell, D., Chateau, M., Karn, J. & Cannon, P. M. HIV-1 infection of microglial cells in a reconstituted humanized mouse model and identification of compounds that selectively reverse HIV latency. *J. Neurovirol.* **24**, 192–203 (2018).
7. Le Douce, V., Cherrier, T., Riclet, R., Rohr, O. & Schwartz, C. The Many lives of CTIP2: From AIDS to cancer and cardiac hypertrophy. *J. Cell. Physiol.* **229**, 533–537 (2014).
8. Le Douce, V. *et al.* HIC1 controls cellular- and HIV-1-gene transcription via interactions with CTIP2 and HMGA1. *Sci. Rep.* **6**, 34920 (2016).
9. Marban, C. *et al.* Recruitment of chromatin-modifying enzymes by CTIP2 promotes HIV-1 transcriptional silencing. *EMBO J.* **26**, 412–423 (2007).
10. Le Douce, V. *et al.* LSD1 cooperates with CTIP2 to promote HIV-1 transcriptional silencing. *Nucleic Acids Res.* **40**, 1904–1915 (2012).
11. Rohr, O. *et al.* Recruitment of tat to heterochromatin protein HP1 via interaction with CTIP2 inhibits human immunodeficiency virus type 1 replication in microglial cells. *J Virol* **77**, 5415–5427 (2003).
12. Cherrier, T. *et al.* CTIP2 is a negative regulator of P-TEFb. *Proc. Natl. Acad. Sci. U.S.A.* **110**, 12655–12660 (2013).
13. Eilebrecht, S. *et al.* HMGA1 recruits CTIP2-repressed P-TEFb to the HIV-1 and cellular target promoters. *Nucleic Acids Res.* **42**, 4962–4971 (2014).
14. Desplats, P. *et al.* Molecular and pathologic insights from latent HIV-1 infection in the human brain. *Neurology* **80**, 1415–1423 (2013).
15. Moosmann, P., Georgiev, O., Le Douarin, B., Bourquin, J. P. & Schaffner, W. Transcriptional repression by RING finger protein TIF1 beta that interacts with the KRAB repressor domain of KOX1. *Nucleic Acids Res.* **24**, 4859–4867 (1996).
16. Iyengar, S. & Farnham, P. J. KAP1 Protein: An enigmatic master regulator of the genome. *J Biol Chem* **286**, 26267–26276 (2011).
17. Iyengar, S., Ivanov, A. V., Jin, V. X., Rauscher, F. J. & Farnham, P. J. Functional analysis of KAP1 genomic recruitment. *Mol. Cell. Biol.* **31**, 1833–1847 (2011).
18. Liang, Q. *et al.* Tripartite motif-containing protein 28 is a small ubiquitin-related modifier E3 ligase and negative regulator of IFN regulatory factor 7. *J. Immunol.* **187**, 4754–4763 (2011).
19. Riclet, R. *et al.* Disruption of the interaction between transcriptional intermediary factor 1β and heterochromatin protein 1 leads to a switch from DNA hyper- to hypomethylation and H3K9 to H3K27 trimethylation on the MEST promoter correlating with gene reactivation. *Mol Biol Cell* **20**, 296–305 (2009).
20. Yang, Y. *et al.* Acetylated hsp70 and KAP1-mediated Vps34 SUMOylation is required for autophagosome creation in autophagy. *Proc. Natl. Acad. Sci. U.S.A.* **110**, 6841–6846 (2013).
21. Garvin, A. J. *et al.* The deSUMOylase SENP7 promotes chromatin relaxation for homologous recombination DNA repair. *EMBO Rep.* **14**, 975–983 (2013).
22. Groh, S. & Schotta, G. Silencing of endogenous retroviruses by heterochromatin. *Cell Mol. Life Sci.* **74**, 2055–2065 (2017).
23. Allouch, A. *et al.* The TRIM family protein KAP1 Inhibits HIV-1 integration. *Cell Host Microbe* **9**, 484–495 (2011).
24. Nishitsuji, H., Abe, M., Sawada, R. & Takaku, H. ZBRK1 represses HIV-1 LTR-mediated transcription. *FEBS Lett.* **586**, 3562–3568 (2012).
25. Nishitsuji, H., Sawada, L., Sugiyama, R. & Takaku, H. ZNF10 inhibits HIV-1 LTR activity through interaction with NF-κB and Sp1 binding motifs. *FEBS Lett.* **589**, 2019–2025 (2015).
26. McNamara, R. P. *et al.* KAP1 recruitment of the 7SK snRNP complex to promoters enables transcription elongation by RNA polymerase II. *Mol. Cell* **61**, 39–53 (2016).
27. Morton, E. L. *et al.* Transcriptional circuit fragility influences HIV proviral fate. *Cell Rep.* **27**, 154-171.e9 (2019).
28. Lee, A., CingÖz, O., Sabo, Y. & Goff, S. P. Characterization of interaction between Trim28 and YY1 in silencing proviral DNA of Moloney murine leukemia virus. *Virology* **516**, 165–175 (2018).
29. Wolf, D. & Goff, S. P. Embryonic stem cells use ZFP809 to silence retroviral DNAs. *Nature* **458**, 1201–1204 (2009).
30. Taura, M., Song, E., Ho, Y.-C. & Iwasaki, A. Apobec3A maintains HIV-1 latency through recruitment of epigenetic silencing machinery to the long terminal repeat. *Proc. Natl. Acad. Sci. U.S.A.* **116**, 2282–2289 (2019).
31. Ma, X. *et al.* TRIM28 promotes HIV-1 latency by SUMOylating CDK9 and inhibiting P-TEFb. *Elife* **8**, e42426 (2019).
32. Wires, E. S. *et al.* Methamphetamine activates nuclear factor kappa-light-chain-enhancer of activated B cells (NF-κB) and induces human immunodeficiency virus (HIV) transcription in human microglial cells. *J. Neurovirol.* **18**, 400–410 (2012).
33. Kutsch, O., Benveniste, E. N., Shaw, G. M. & Levy, D. N. Direct and quantitative single-cell analysis of human immunodeficiency virus type 1 reactivation from latency. *J. Virol.* **76**, 8776–8786 (2002).
34. Meylan, S. *et al.* A gene-rich, transcriptionally active environment and the pre-deposition of repressive marks are predictive of susceptibility to KRAB/KAP1-mediated silencing. *BMC Genomics* **12**, 378 (2011).
35. Ryan, R. F. *et al.* KAP-1 corepressor protein interacts and colocalizes with heterochromatic and euchromatic HP1 proteins: a potential role for Krüppel-associated box-zinc finger proteins in heterochromatin-mediated gene silencing. *Mol. Cell. Biol.* **19**, 4366–4378 (1999).
36. Coiras, M. *et al.* Modifications in the human T cell proteome induced by intracellular HIV-1 Tat protein expression. *Proteomics* **6**, S63–S73 (2006).
37. Ruben, S. *et al.* Structural and functional characterization of human immunodeficiency virus tat protein. *J. Virol.* **63**, 1–8 (1989).
38. Ali, A. & Banerjea, A. C. Curcumin inhibits HIV-1 by promoting Tat protein degradation. *Sci Rep* **6**, 27539 (2016).
39. Balachandran, A. *et al.* Identification of small molecule modulators of HIV-1 Tat and Rev protein accumulation. *Retrovirology* **14**, 7 (2017).
40. Gargano, B., Fiorillo, M., Amente, S., Majello, B. & Lania, L. p14ARF is capable of promoting HIV-1 tat degradation. *Cell Cycle* **7**, 1433–1439 (2008).
41. Hong, H.-W., Lee, S.-W. & Myung, H. Induced degradation of Tat by nucleocapsid (NC) via the proteasome pathway and its effect on HIV transcription. *Viruses* **5**, 1143–1152 (2013).
42. Li, J. *et al.* Long noncoding RNA NRON contributes to HIV-1 latency by specifically inducing tat protein degradation. *Nat. Commun.* **7**, 11730 (2016).
43. Wan, Z. & Chen, X. Triptolide inhibits human immunodeficiency virus type 1 replication by promoting proteasomal degradation of Tat protein. *Retrovirology* **11**, 88 (2014).
44. Sacco, A. *et al.* Carfilzomib-dependent selective inhibition of the chymotrypsin-like activity of the proteasome leads to antitumor activity in Waldenstrom's Macroglobulinemia. *Clin Cancer Res* **17**, 1753–1764 (2011).
45. Li, X. *et al.* Role for KAP1 serine 824 phosphorylation and sumoylation/desumoylation switch in regulating KAP1-mediated transcriptional repression. *J. Biol. Chem.* **282**, 36177–36189 (2007).
46. Ivanov, A. V. *et al.* PHD domain-mediated E3 ligase activity directs intramolecular sumoylation of an adjacent bromodomain required for gene silencing. *Mol. Cell* **28**, 823–837 (2007).

47. Cheng, C.-T., Kuo, C.-Y. & Ann, D. K. KAPtain in charge of multiple missions: Emerging roles of KAP1. *World J Biol Chem* **5**, 308–320 (2014).
48. Cismasiu, V. B. *et al.* BCL11B is a general transcriptional repressor of the HIV-1 long terminal repeat in T lymphocytes through recruitment of the NuRD complex. *Virology* **380**, 173–181 (2008).
49. Schultz, D. C., Friedman, J. R. & Rauscher, F. J. Targeting histone deacetylase complexes via KRAB-zinc finger proteins: the PHD and bromodomains of KAP-1 form a cooperative unit that recruits a novel isoform of the Mi-2alpha subunit of NuRD. *Genes Dev.* **15**, 428–443 (2001).
50. Quénet, D. *et al.* The histone subcode: poly(ADP-ribose) polymerase-1 (Parp-1) and Parp-2 control cell differentiation by regulating the transcriptional intermediary factor TIF1beta and the heterochromatin protein HP1alpha. *FASEB J.* **22**, 3853–3865 (2008).
51. Tomimatsu, N., Mukherjee, B. & Burma, S. Distinct roles of ATR and DNA-PKcs in triggering DNA damage responses in ATM-deficient cells. *EMBO Rep.* **10**, 629–635 (2009).
52. Cherrier, T. *et al.* p21(WAF1) gene promoter is epigenetically silenced by CTIP2 and SUV39H1. *Oncogene* **28**, 3380–3389 (2009).
53. Imai, K. *et al.* Cyclin T1 stabilizes expression levels of HIV-1 Tat in cells. *FEBS J.* **276**, 7124–7133 (2009).
54. Jin, X. *et al.* MAGE-TRIM28 complex promotes the Warburg effect and hepatocellular carcinoma progression by targeting FBP1 for degradation. *Oncogenesis* **6**, e312 (2017).
55. Okamoto, K., Kitabayashi, I. & Taya, Y. KAP1 dictates p53 response induced by chemotherapeutic agents via Mdm2 interaction. *Biochem. Biophys. Res. Commun.* **351**, 216–222 (2006).
56. Pineda, C. T. *et al.* Degradation of AMPK by a cancer-specific ubiquitin ligase. *Cell* **160**, 715–728 (2015).
57. Avram, D. & Califano, D. The multifaceted roles of Bcl11b in thymic and peripheral T cells - impact on immune diseases. *J Immunol* **193**, 2059–2065 (2014).
58. Czerwińska, P., Mazurek, S. & Wiznerowicz, M. The complexity of TRIM28 contribution to cancer. *J Biomed Sci* **24**, 63 (2017).
59. Czerwińska, P. *et al.* TRIM28 multi-domain protein regulates cancer stem cell population in breast tumor development. *Oncotarget* **8**, 863–882 (2017).
60. Hu, M. *et al.* Expression of KAP1 in epithelial ovarian cancer and its correlation with drug-resistance. *Int. J. Clin. Exp. Med.* **8**, 17308–17320 (2015).
61. Wang, Y.-Y., Li, L., Zhao, Z.-S. & Wang, H.-J. Clinical utility of measuring expression levels of KAP1, TIMP1 and STC2 in peripheral blood of patients with gastric cancer. *World J. Surg. Oncol.* **11**, 81 (2013).
62. Janabi, N., Peudenier, S., Héron, B., Ng, K. H. & Tardieu, M. Establishment of human microglial cell lines after transfection of primary cultures of embryonic microglial cells with the SV40 large T antigen. *Neurosci. Lett.* **195**, 105–108 (1995).

Acknowledgement

We thank Dr. David K. Ann, Dr. Ivan D'orso and Dr. Florence Cammas for providing vectors. We thank participants to the ANRS (French National Agency for Research on AIDS and Viral Hepatitis) RHIVIERA (Remission of HIV Era) Consortium for helpful discussion.

Author contributions

Conceived and designed the experiments: O.R., C.V.L. and V.G. Performed the experiments: A.A.A., M.B. and F.D. Analyzed the data: O.R., C.V.L., V.G., A.A.A., M.B., F.D., V.M., J.V.A., C.W., A.R., M.D.R., B.F. and C.S. Wrote the paper: A.A.A. and O.R.

Funding

This work was supported by the French agency for research on AIDS and viral hepatitis (ANRS); SIDACTION; the European Union's Horizon 2020 research and innovation programme under grant agreement No 691119-EU4HIVCURE-H2020-MSCA-RISE-2015; RHIVIERA; The Belgian Fund for Scientific Research (FRS-FNRS, Belgium), the "Fondation Roi Baudouin", the Walloon Region (Fonds de Maturation) and the university of Brussels (Action de Recherche Concertée (ARC) grant). The laboratory of CVL is part of the ULB-Cancer Research Centre (U-CRC). AAA is a fellow of the Wallonie-Bruxelles International program and of the Marie Skłodowska Curie COFUND action. MB is a doctoral fellow from the Belgian Fonds pour la formation à la Recherche dans l'Industrie et dans l'Agriculture (FRIA). CVL is Directeur de Recherches of the F.R.S-FNRS, Belgium. AR is funded by a postdoctoral fellowship from the Université Libre de Bruxelles (ULB) - Action de Recherche Concertée (ARC) program (2016-2021 grant). We thank ViiV Healthcare.

Competing interests

The authors declare no competing interests.

Additional information

Supplementary Information The online version contains supplementary material available at https://doi.org/10.1038/s41598-021-82164-w.

Correspondence and requests for materials should be addressed to C.L., V.G. or O.R.

Reprints and permissions information is available at www.nature.com/reprints.

Publisher's note Springer Nature remains neutral with regard to jurisdictional claims in published maps and institutional affiliations.